BIOCHEMISTRY
including biophysical chemistry & molecular biology

Article

pubs.acs.org/biochemistry

# Protein-Bound Water as the Determinant of Asymmetric Functional Conversion between Light-Driven Proton and Chloride Pumps

Kosuke Muroda,[†] Keisuke Nakashima,[†] Mikihiro Shibata,[†] Makoto Demura,[‡] and Hideki Kandori*,[†]

[†]Department of Frontier Materials, Nagoya Institute of Technology, Showa-ku, Nagoya 466-8555, Japan

[‡]Division of Biological Sciences, Graduate School of Science, Hokkaido University, Sapporo 060-8602, Japan

Supporting Information

**ABSTRACT:** Bacteriorhodopsin (BR) and halorhodopsin (HR) are light-driven outward proton and inward chloride pumps, respectively. They have similar protein architecture, being composed of seven-transmembrane helices that bind an all-*trans*-retinal. BR can be converted into a chloride pump by a single amino acid replacement at position 85, suggesting that BR and HR share a common transport mechanism, and the ionic specificity is determined by the amino acid at that position. However, HR cannot be converted into a proton pump by the corresponding reverse mutation. Here we mutated 6 and 10 amino acids of HR into BR-like, whereas such multiple HR mutants never pump protons. Light-induced Fourier transform infrared spectroscopy revealed that hydrogen bonds of the retinal Schiff base and water are both strong for BR and both weak for HR. Multiple HR mutants exhibit strong hydrogen bonds of the Schiff base, but the hydrogen bond of water is still weak. We concluded that the cause of nonfunctional conversion of HR is the lack of strongly hydrogen-bonded water, the functional determinant of the proton pump.

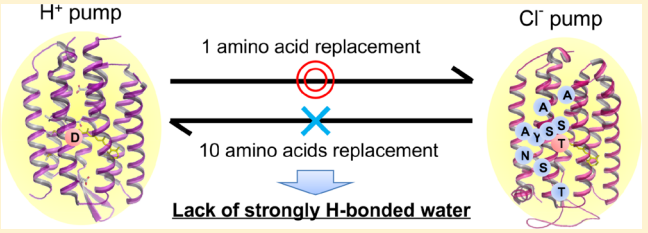


Optogenetics, which utilizes ion-transporting microbial rhodopsins as the tools for controlling light, has revolutionized neuroscience.[1,2] Channelrhodopsin,[2,3] light-gated ion channel, is used to excite neurons by light, while light-driven ion pumps such as bacteriorhodopsin (BR) and halorhodopsin (HR) are used for neural silencing.[4,5] BR and HR function as light-driven outward proton and inward chloride pumps, respectively.[6−9] The chromophore of these proteins is all-*trans*-retinal that binds to a lysine residue through a Schiff base linkage (Figure 1a,b), and the all-*trans*−13-*cis* photoisomerization triggers the pumping process.[10] In spite of different functions and limited amino acid identity (25%), X-ray crystallographic structures showed that BR and HR possess a common protein architecture.[11−13] In fact, peptide backbones of seven transmembrane helices can be superimposed with each other (Figure 1c,d). These structural aspects suggest that BR and HR have been optimized for their own functions by tuning the fine structure during evolution.

Functional conversion using site-directed mutagenesis is one of the suitable methods for elucidating the molecular mechanism of proton and chloride pumps. In 1995, Sasaki et al. succeeded in converting BR into a chloride pump by a single amino acid replacement of Asp85 with Thr, the corresponding amino acid in HR (Figure 1).[14] This fact suggests that BR and HR share a common transport mechanism and the ionic specificity is determined by the amino acid at position 85 (BR numbering). Following structural analysis by X-ray crystallography[15] and Fourier transform infrared (FTIR) spectroscopy[16] of the D85S protein (higher halide binding affinity for Ser than for Thr) provided structural elements for the chloride pump. In contrast, interestingly, the reverse T-to-D mutation of HR, such as the T108D mutant of *Halobacterium salinarum* HR (*s*HR) and the T126D mutant of *Natronomonas pharaonis* HR (*p*HR), never converted HR into the BR-like outward proton pump.[17,18] It is known that in the presence of azide, HR can pump protons outwardly even without any mutation, but the T-to-D mutation is not sufficient for HR to act as the outward proton pump.[18] This fact implies that the molecular design of the proton pump may be more difficult than that of the chloride pump. Although a common mechanism have been considered for light-driven proton and chloride pumps,[6,18−20] this asymmetric functional conversion has been a long-standing mystery. How is this fact explained by structural terms?

In this paper, to examine the detailed functional conversion of HR, we designed two multiple mutants of *p*HR that have six mutations ($p$HR$_6$) and ten mutations ($p$HR$_{10}$) on the basis of the sequential conservation of each pump (Figure S1 of the Supporting Information). Figure 1d shows that Asp85, Asp96, and Glu204 constitute the proton pathway in BR, whose corresponding residues are Thr126, Ala137, and Thr244 of *p*HR, respectively (Figure 1c). We thus introduced the BR-like carboxylates into the multiple *p*HR mutants. In addition, BR-like proton pumps possess three conserved amino acids along the proton pathway, Ala53, Thr89, and Gly220, which correspond to Ser78, Ser130, and Ala260 of *p*HR, respectively (Figure 1c,d and Figure S1 of the Supporting Information).

**Received:** April 15, 2012
**Revised:** May 13, 2012
**Published:** May 14, 2012

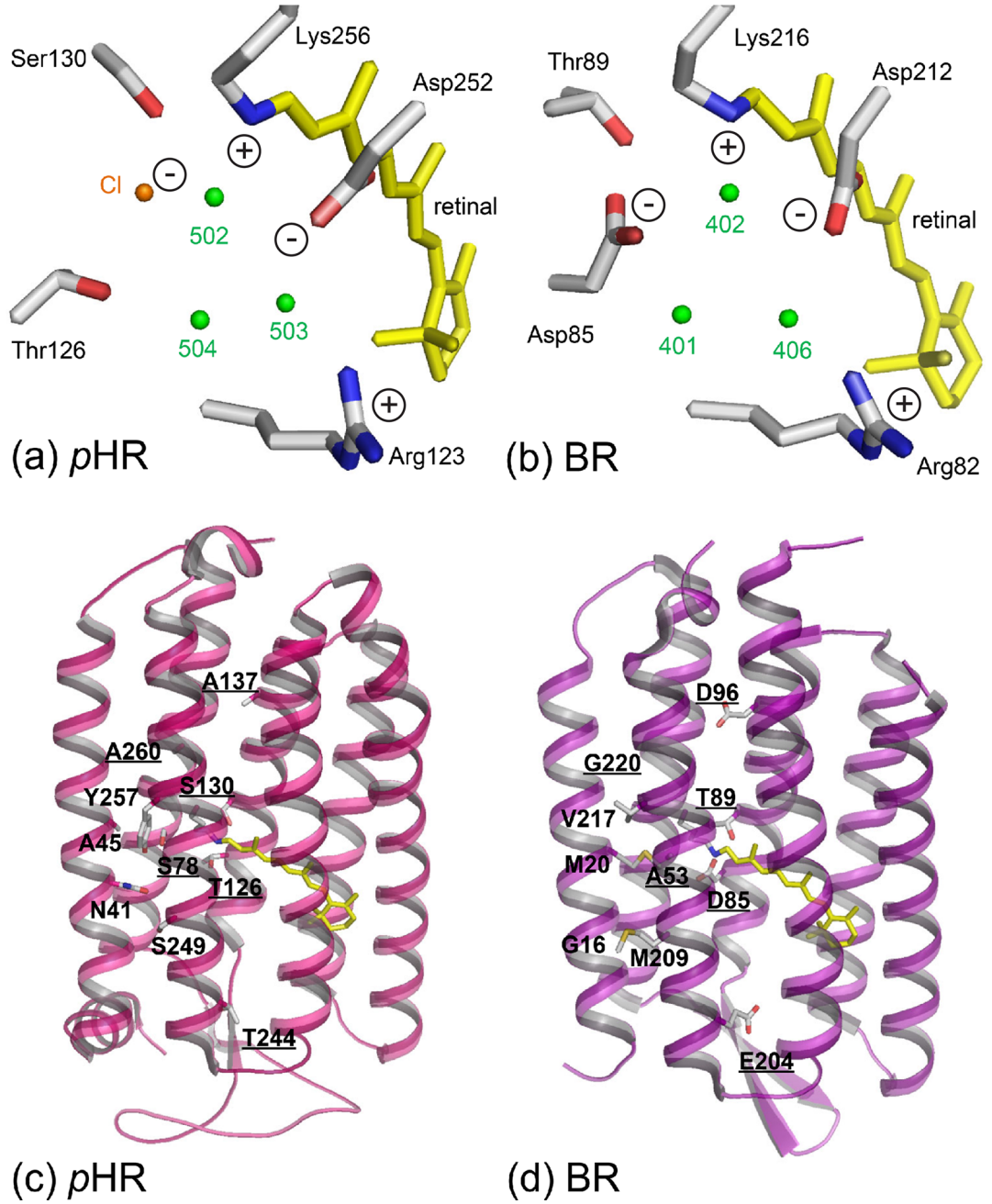


**Figure 1.** X-ray crystallographic structures of *p*HR [a and c; Protein Data Bank (PDB) entry 3A7K][13] and BR (b and d; PDB entry 1C3W).[11] The membrane normal is approximately in the vertical direction, and upper and lower regions correspond to the cytoplasmic (CP) and extracellular (EC) sides, respectively. Green spheres in panels a and b represent water molecules bound inside each protein. In $pHR_6$ (S78A/T126D/S130T/A137D/T244E/A260G), six underlined amino acids of *p*HR (c) are mutated to the corresponding amino acids of BR (underlined in panel d). In $pHR_{10}$ (N41G/A45M/S78A/T126D/S130T/A137D/T244E/S249M/Y257V/A260G), 10 amino acids of *p*HR (c) are mutated to the corresponding amino acids of BR (d).

Thus, we first designed $pHR_6$ (S78A/T126D/S130T/A137D/T244E/A260G). We also focused on the Schiff base region, whose hydrogen bonding network must be important for the proton pumping function. BR-like proton pumps have four conserved amino acids in the Schiff base region, Gly16, Met20, Met209, and Val217, which correspond to Asn41, Ala45, Ser249, and Tyr257 of *p*HR, respectively (Figure 1c,d and Figure S1 of the Supporting Information). We therefore designed $pHR_{10}$ (N41G/A45M/S78A/T126D/S130T/A137D/T244E/S249M/Y257V/A260G). We expected that $pHR_6$ and $pHR_{10}$ pump protons, because they contain BR-like characteristic amino acids.

## MATERIALS AND METHODS

**Sample Preparation.** Expression plasmids for the wild-type *p*HR, T126D *p*HR, $pHR_6$, and $pHR_{10}$ with a six-histidine tag at the C-terminus were constructed as described previously.[21,22] The purification of proteins is essentially the same as that described in the previous reports.[21−23] Briefly, *Escherichia coli* BL21(DE3) cells containing the plasmid of each protein were grown at 38 °C in 2× YT medium supplemented


dx.doi.org/10.1021/bi300485r | *Biochemistry* 2012, 51, 4677−4684

with 50 μg/mL ampicillin. At an $OD_{660}$ of 0.5−0.6, 1 mM IPTG (isopropyl 1-thio-β-galactoside) and 10 μM all-*trans*-retinal were added, and after 3 h, cells were harvested. The *E. coli* cells were directly used for the ion-transport experiments. The [ζ-$^{15}$N]Lys-labeled sample was grown in M9 medium, where 50 mg/L labeled L-lysine (Isotech) was added to the medium as described previously.[23,24]

For the spectroscopic measurements, pink colored cells 3 h after the IPTG induction were sonicated, solubilized with 1.0% *n*-dodecyl β-D-maltoside, and purified via Ni-NTA affinity chromatography and DEAE (diethylaminoethyl) ion exchange chromatography. Each absorption spectrum (Figure 2, left) was measured in elution buffer [50 mM Tris, 300 mM NaCl, 300 mM imidazole, and 0.1% *n*-dodecyl β-D-maltopyranoside (pH 7.0)]. To measure the dependence of salt (Figure 2, right), we dialyzed each sample in a 50 mM phosphate buffer containing 0.1% *n*-dodecyl β-D-maltopyranoside at pH 7.0, in the absence and presence of 150 mM NaCl.

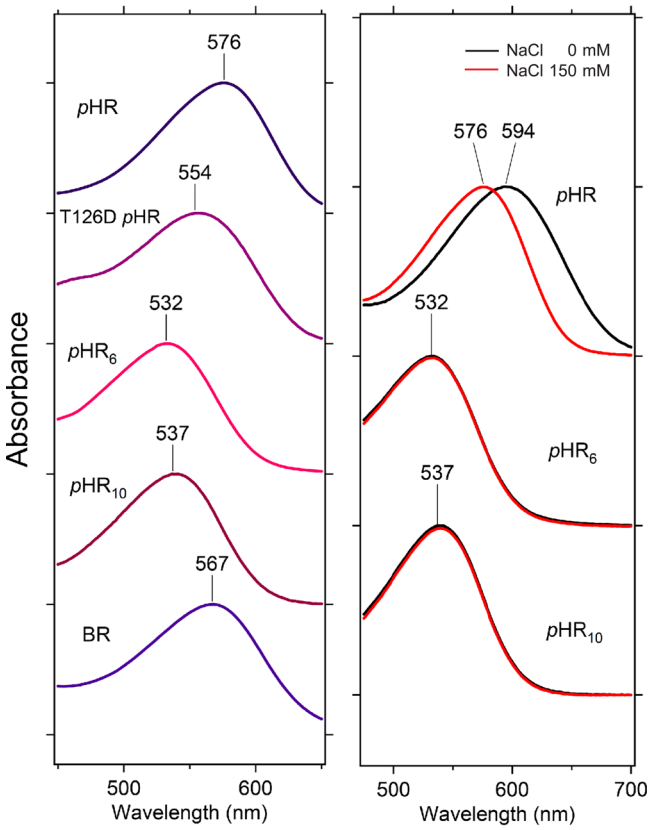


**Figure 2.** Absorption spectra of wild-type and mutant *p*HR in the dark measured for the detergent-solubilized sample [0.1% dodecyl maltoside (pH 7.0)] at 20 °C. Absorption spectra (left) of wild-type *p*HR, T126D *p*HR, $pHR_6$, $pHR_{10}$, and BR (from top to bottom, respectively) in Tris buffer [50 mM Tris, 300 mM NaCl, 300 mM imidazole, and 0.1% dodecyl maltoside (pH 7.0)]. Salt dependence (right) of the absorption spectra of wild-type *p*HR, $pHR_6$, and $pHR_{10}$ (from top to bottom, respectyively). Black and red curves represent the spectra in the absence and presence, respectively, of 150 mM NaCl in phosphate buffer [50 mM phosphate and 0.1% dodecyl maltoside (pH 7.0)].

For low-temperature UV−visible and FTIR spectroscopy, wild-type and mutant *p*HR were reconstituted into L-α-phosphatidylcholine liposomes by the removal of the detergent with Biobeads, where the molar ratio of the added lipid to protein was 50:1. The *p*HR samples in PC liposomes were washed twice with buffers at pH 7.0 (2 mM phosphate and 5 mM NaCl).

**Ion-Transport Measurements.** Ion-transport measurements were performed by using a pH electrode as described previously.[25,26] The *E. coli* cells were washed three times with a solution containing 50 mM $MgSO_4$ and 300 mM NaCl. Changes in pH in the suspension of the *E. coli* cells containing each *p*HR protein were measured with a glass electrode under illumination at >500 nm (25 °C) by use of a HORIBA F-55 pH meter, where the initial pH was adjusted to ∼7. The samples were then illuminated after addition of CCCP to a final concentration of 10 μM. The light source for illumination was a slide projector with 1 kW tungsten lamp through optical filters.

**UV−Visible Spectroscopy.** Absorption spectra were recorded for the protein in 0.1% dodecyl maltoside (pH 7) at 20 °C using a UV-2400PC (Shimadzu) spectrometer.[27] For low-temperature difference UV−visible spectroscopy, we prepared hydrated films as described previously,[28] and this method was also used for low-temperature difference FTIR spectroscopy. The sample film was prepared by drying the protein in 2 mM phosphate buffer (pH 7.0) on a $BaF_2$ window with a diameter of 18 mm, which was then rehydrated with 1 μL of $H_2O$, and the window was mounted in an Oxford DN-1704 cryostat. Light-minus-dark difference UV−visible spectra were recorded with a V-550DS (Jasco) spectrometer, in which samples were illuminated at >500 nm (Y52 glass filter) with a slide projector with a 1 kW tungsten lamp. We tested the temperature range of 220−270 K.

**Low-Temperature FTIR Spectroscopy.** Light-induced difference FTIR spectroscopy at 77 K was performed as described previously.[23,28] After hydration with $H_2O$, $D_2O$, or $D_2{}^{18}O$, the sample was placed in a cell, which was mounted in an Oxford Optistat-DN cryostat placed in a DIGILAB FTS 40 or 7000 spectrometer. All spectra were measured at 2 $cm^{-1}$ resolution. The K-minus-*p*HR difference spectra were measured as follows. Illumination of the *p*HR film at pH 7 with 500 nm light at 77 K for 2 min converted *p*HR to the K intermediate. The difference spectrum was calculated from spectra constructed with 256 interferograms collected before and after the illumination. At least three spectra obtained in this way were averaged for the K-minus-*p*HR spectra.

## RESULTS

**Visible Absorption and Proton-Transport Properties of the HR Mutants.** *p*HR and BR exhibit similar absorption; their $\lambda_{max}$ values are located at 576 and 567 nm at neutral pH, respectively (Figure 2, left). Absorptions of the *p*HR mutants are all blue-shifted, the $\lambda_{max}$ values being 554, 532, and 537 nm for T126D, $pHR_6$, and $pHR_{10}$, respectively. The absorption spectra of wild-type *p*HR differ in the absence ($\lambda_{max}$ = 594 nm) and presence ($\lambda_{max}$ = 576 nm) of chloride (Figure 2, right). This shows that chloride acts as the Schiff base counterion as shown in Figure 1a. In contrast, addition of chloride (at pH 7.0) to $pHR_6$ and $pHR_{10}$ does not shift the absorption spectra at all (Figure 2, right), implying no binding of chloride near the Schiff base region. This suggests that Asp126 functions as the counterion in $pHR_6$ and $pHR_{10}$, like Asp85 in BR.

We then measured light-driven ion transport by monitoring the pH changes with a glass electrode. Figure 3 shows light-induced pH changes in *E. coli* cells containing each HR protein, where the amounts of protein in suspension are equal. In the case of wild-type *p*HR, illumination caused a net alkalization of


dx.doi.org/10.1021/bi300485r | *Biochemistry* 2012, 51, 4677−4684

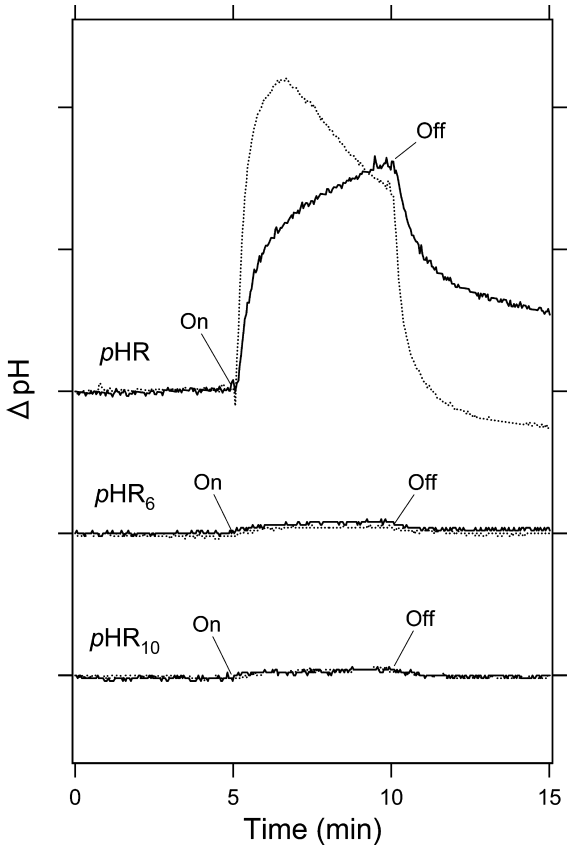


**Figure 3.** Time course of light-induced pH changes in *E. coli* cells containing wild-type *p*HR (top), *p*HR$_6$ (middle), and *p*HR$_{10}$ (bottom). On and Off indicate the onset and offset of illumination (with yellow light, >500 nm), respectively, and a positive signal corresponds to a decrease in pH (alkalization). The amount of protein in the suspension is made equal using its absorption, so that the same amount of protein is responsible for ion transport. Dotted lines represent identical measurements in the presence of 10 $\mu$M CCCP. One division of the *y*-axis corresponds to 0.125 pH unit.

the medium, which is further increased by addition of a protonophore, 10 $\mu$M CCCP. This is characteristic of HR, an inward chloride pump. In contrast, illumination of *p*HR$_6$ and *p*HR$_{10}$ does not cause any pH changes (Figure 3), indicating that *p*HR$_6$ and *p*HR$_{10}$ do not pump protons. While BR is converted into a chloride pump by a single amino acid replacement,[14] *p*HR cannot be converted into a proton pump even by introduction of multiple mutations at positions 6 and 10. In the case of D85T and D85S BR, a transported chloride is bound to the Schiff base region, and light-induced structural changes cause unidirectional movement of chloride. Similarly, the appearance of visible absorption at 500−550 nm (Figure 2) clearly shows that a transported proton is bound to the Schiff base. Nevertheless, light-induced structural changes do not cause unidirectional movement of the proton. Below we study the cause of such asymmetric functional conversion between proton and chloride pumps by use of low-temperature UV−visible and FTIR spectroscopy.

**Low-Temperature UV−Visible Spectroscopy of HR Mutants.** For the proton pumping function, the transfer of a proton from the retinal Schiff base to its acceptor is a prerequisite. The deprotonated Schiff base possesses highly blue-shifted absorption, whose maximum is located at 360−410 nm. Therefore, UV−visible absorption spectroscopy can be used to monitor deprotonation of the Schiff base. Figure S2 of the Supporting Information clearly shows the formation of a deprotonated Schiff base in BR ($\lambda_{max}$ = 412 nm), which corresponds to the formation of the M intermediate. On the other hand, the Schiff base is never deprotonated for HR, and Figure S2a of the Supporting Information shows that the photoproduct of wild-type *p*HR is the L intermediate ($\lambda_{max}$ = 496 nm) at 230 K. The photoproduct of T126D *p*HR is similarly the L intermediate ($\lambda_{max}$ = 472 nm) at 230 K as well as the wild type. In the case of *p*HR$_6$ and *p*HR$_{10}$, red-shifted intermediates appear over the wide temperature range between 220 and 270 K. Thus, the Schiff base is never deprotonated during the photocycles of T126D *p*HR, *p*HR$_6$, and *p*HR$_{10}$, being consistent with no proton pumping activity. It is known that azide assists in the proton transport of HR even for the wild type,[18,20,28] in which azide probably lowers the difference in p$K_a$ transiently and thus facilitates proton transfer reactions for unidirectional transport. However, introduction of multiple mutations into *p*HR is not sufficient for the primary proton transfer.

**Structural Analysis of the Schiff Base Region of the HR Mutants Using Low-Temperature FTIR Spectroscopy.** Visible spectral analysis suggests that newly introduced Asp126 is deprotonated in *p*HR$_6$ and *p*HR$_{10}$ and acts as the Schiff base counterion like Asp85 in BR. Nevertheless, *p*HR$_6$ and *p*HR$_{10}$ exhibit neither proton pumping activity nor Schiff base deprotonation. These observations suggest that *p*HR$_6$ and *p*HR$_{10}$ still do not become BR-like, and introduction of 6 or 10 amino acids is not sufficient to pump protons. To further study the structural feature, we measured difference FTIR spectra of *p*HR$_6$ and *p*HR$_{10}$. Figure S3 of the Supporting Information compares K-minus-BR difference spectra in the 1800−800 cm$^{-1}$ region measured in $H_2O$ at 77 K, which monitors local structures around the retinal chromophore after and before retinal photoisomerization. One characteristic aspect of HR is that the ethylenic C=C stretching vibration of the retinal chromophore (1550−1500 cm$^{-1}$) is upshifted,[23,29,30] though all other rhodopsins show a downshifted band because of the red shift in the visible region. Figure S3 of the Supporting Information shows that T126D *p*HR [1538 (+)/1527 (−) cm$^{-1}$] is upshifted as well as wild-type *p*HR [1538 (+)/1527 (−) cm$^{-1}$]. In contrast, *p*HR$_6$ [1541 (−)/1527 (+) cm$^{-1}$] and *p*HR$_{10}$ [1536 (−)/1527 (+) cm$^{-1}$] exhibit downshifted C=C stretches like BR [1530 (−)/1514 (+) cm$^{-1}$]. This spectral feature indicates that *p*HR$_6$ and *p*HR$_{10}$ become BR-like. In the frequency region of 1250−1200 cm$^{-1}$ (C−C stretching vibrations of the retinal chromophore), *p*HR shows characteristic negative peaks at 1257, 1244, and 1210 cm$^{-1}$, while BR has peaks at 1255 and 1203 cm$^{-1}$ (Figure S3 of the Supporting Information). The spectral feature of T126D *p*HR is entirely HR-like. In contrast, *p*HR$_6$ and *p*HR$_{10}$ possess a single negative peak at 1253 cm$^{-1}$ like BR, not two peaks at 1257 and 1244 cm$^{-1}$. In addition, *p*HR$_{10}$ exhibits the BR-like peak pair at 1202 (−)/1196 (+) cm$^{-1}$. This implies that the chromophore structure becomes BR-like, especially in the case of *p*HR$_{10}$.

We next examined a higher-frequency region, in which the N−D stretch of the Schiff base and O−D stretches of water can be measured in $D_2O$. It is known that the hydrogen bond of the Schiff base is very strong in BR, but not in HR. Most microbial rhodopsins possess Schiff base N−D stretches at 2180−2080 cm$^{-1}$, which have also been identified for BR,[31] *pharaonis* sensory rhodopsin II (*p*SRII),[32] proteorhodopsin (PR),[33] *Anabaena* sensory rhodopsin (ASR),[34] and *Gloeobacter*


dx.doi.org/10.1021/bi300485r | *Biochemistry* 2012, 51, 4677−4684

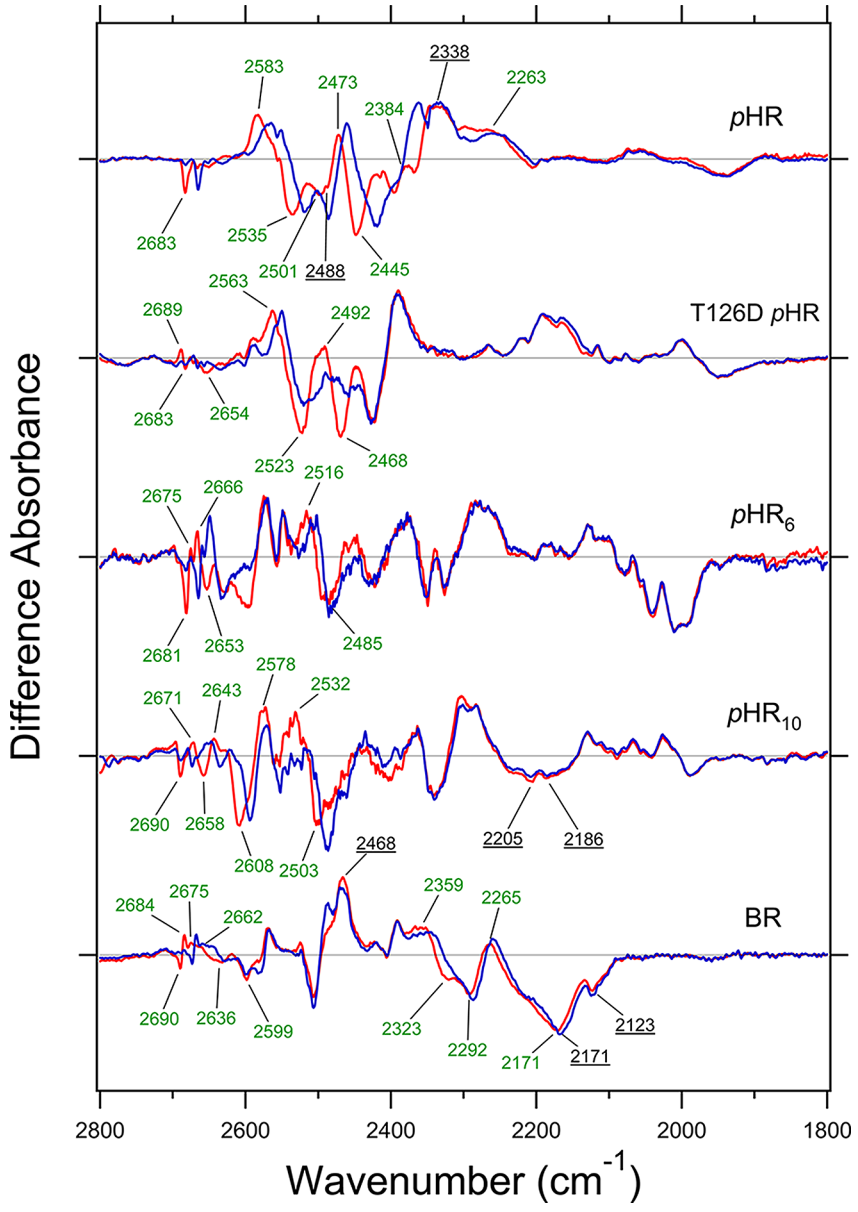


**Figure 4.** Light-minus-dark difference FTIR spectra of wild-type *p*HR, T126D *p*HR, $pHR_6$, $pHR_{10}$, and BR (from top to bottom, respectively) in the 2800−1800 $cm^{-1}$ region. The samples were hydrated with $D_2O$ (red curves) or $D_2{}^{18}O$ (blue curves), and spectra were recorded by illumination with a 500 nm light (through an interference filter) for 2 min at 77 K. Frequencies labeled in green correspond to those identified as O−D stretching vibrations of water. Underlined frequencies also contain the N−D stretch of the Schiff base. One division of the *y*-axis corresponds to 0.0015 absorbance unit. The spectra of $pHR_{10}$ are shown without a change in amplitude, while those of wild-type *p*HR, T126D *p*HR, $pHR_6$, and BR are multiplied by factors of 0.80, 0.64, 3.16, and 0.31, respectively. The data for wild-type *p*HR and BR are reproduced from refs 23 and 36, respectively.

rhodopsin (GR)[35] by use of [$\zeta$-$^{15}$N]Lys-labeled samples. In contrast, the N−D stretch appears at 2488 $cm^{-1}$ for *p*HR, a >300 $cm^{-1}$ higher frequency that is characteristic for HR.[23] Figure S4 of the Supporting Information shows the spectral comparison between unlabeled and [$\zeta$-$^{15}$N]Lys-labeled samples in the 2300−1850 $cm^{-1}$ region, confirming no Schiff base vibration for *p*HR and negative bands at 2171 and 2123 $cm^{-1}$ due to the Schiff base N−D stretch in BR. Figure S4 of the Supporting Information clearly shows that the negative bands at 2205 and 2186 $cm^{-1}$ in $pHR_{10}$ exhibit isotope shifts. This clearly indicates that $pHR_{10}$ becomes BR-like in terms of the strong hydrogen bond of the Schiff base, but $pHR_{10}$ does not pump protons.

We then compared O−D stretches of water in $D_2O$ (Figure 4). BR possesses three water O−D stretching vibrations below 2400 $cm^{-1}$ (negative bands at 2323, 2292, and 2171 $cm^{-1}$)[36] as well as the Schiff base N−D stretch,[31] indicating that hydrogen bonds of the Schiff base and water are both strong. In contrast, *p*HR in the unphotolyzed state possesses neither a Schiff base N−D stretch nor water O−D stretches below 2400 $cm^{-1}$,[23] indicating that hydrogen bonds of the Schiff base and water are both weak. Figure 4 clearly shows that water bands appear only above 2400 $cm^{-1}$ for T126D *p*HR, $pHR_6$, and $pHR_{10}$, indicating that hydrogen bonds of water are weak for these proteins.

## DISCUSSION

X-ray crystallography visualized the presence of protein-bound water molecules in light-driven ion pumps (Figure 1).[11,13] On the other hand, their functional role has been extensively


dx.doi.org/10.1021/bi300485r | *Biochemistry* 2012, 51, 4677−4684

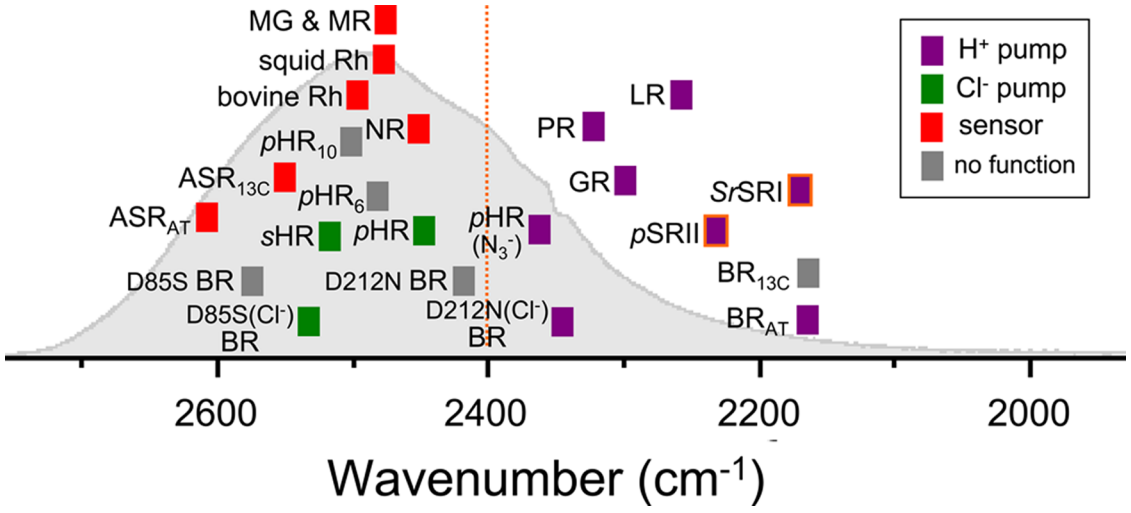


**Figure 5.** In the light-induced difference FTIR spectra of various rhodopsins at 77 K, the lowest frequency among the observed water O−D stretching vibrations is plotted. Purple squares represent the results for the proton pump, while red and green squares are those for the sensor and chloride pump, respectively. The proteins denoted with dark gray squares have no function. Abbreviations: $BR_{AT}$, BR containing all-*trans*-retinal;[36] $BR_{13C}$, BR containing 13-*cis*-retinal;[52] D85S BR;[16] D85S($Cl^-$) BR;[16] D212N BR;[53] D212N($Cl^-$) BR;[53] *Sr*SRI, *Salinibacter ruber* sensory rhodopsin I;[54] *p*SRII, *N. pharaonis* sensory rhodopsin II;[55] LR, *Leptosphaeria* rhodopsin;[56] GR, *Gloeobacter* rhodopsin;[35] PR, proteorhodopsin;[33] $ASR_{AT}$, *Anabaena* sensory rhodopsin containing all-*trans*-retinal;[47] $ASR_{13C}$, *Anabaena* sensory rhodopsin containing 13-*cis*-retinal;[34] NR, *Neurospora* rhodopsin;[48] bovine Rh, bovine rhodopsin;[57] squid Rh, squid rhodopsin;[58] MG and MR, monkey green- and red-sensitive visual pigments, respectively;[59] *s*HR, *H. salinarum* halorhodopsin;[60] *p*HR, *N. pharaonis* halorhodopsin;[23] *p*HR($N_3^-$), *N. pharaonis* halorhodopsin that binds azide;[28] $pHR_6$, sextet mutant of *N. pharaonis* halorhodopsin; $pHR_{10}$, 10-residue mutant of *N. pharaonis* halorhodopsin. SRI and SRII are sensors, but it is known that they pump protons in the absence of transducer proteins (purple squares with orange frames).[43,44] The light gray spectrum shows the water O−D stretching vibration, and only proton-pumping rhodopsins possess strongly hydrogen bonded waters (O−D stretch below 2400 $cm^{-1}$).

studied by light-induced difference FTIR spectroscopy. Using time-resolved FTIR spectroscopy, Gerwert and co-workers revealed the dynamics of protein-bound water molecules in BR.[37−39] We applied low-temperature FTIR spectroscopy to BR and other rhodopsins.[40,41] Difference FTIR spectroscopy further elucidated the functional correlation with the water hydrogen bond. From the comprehensive studies of water vibrations of various rhodopsins, we found that strongly hydrogen bonded water molecules (O−D stretch below 2400 $cm^{-1}$ in $D_2O$) are always present in the rhodopsins exhibiting proton pumping activity.[10] Figure 5 illustrates such a functional correlation between hydrogen bonding strength of water and rhodopsin function, where we plot the lowest-frequency band of water for the unphotolyzed state in $D_2O$. Because the measurements were performed at 77 K, protein-bound water molecules near the retinal chromophore must be detected. In particular, water molecules in the Schiff base region are good candidates for the lowest-frequency band of water, because the other part of retinal is hydrophobic. The Schiff base region contains negative charges such as carboxylates and chloride (Figure 1a,b), which is the reasonable acceptor of the strong hydrogen bond of water. In fact, using comprehensive mutations, we identified strongly hydrogen bonded water in BR being directly hydrogen bonded to Asp85 and Asp212,[36] a finding also supported by the QM/MM calculation.[42]

Figure 5 shows that the rhodopsins exhibiting proton pumping activity possess water O−D stretching vibrations below 2400 $cm^{-1}$. In contrast, the lowest water O−D stretching vibrations of chloride pump and sensor proteins are above 2400 $cm^{-1}$. It should be noted that SRI and SRII function as sensors, not pumps, but they pump protons in the absence of their transducer proteins.[43,44] Thus, the strong correlation between water hydrogen bond and proton pumping function led us to conclude that a protein-bound water molecule is the functional determinant of the proton pump. This observation is also consistent with our discovery, as $pHR_6$ and $pHR_{10}$ do not pump protons and possess no strongly hydrogen bonded waters. The strong hydrogen bond of the Schiff base in $pHR_{10}$ (Figure S4 of the Supporting Information) indicates that this 10-residue mutant *p*HR becomes BR-like, but that is not the case for its protein-bound water molecules. It appears that this mutant wants to pump protons, whereas water does not permit it.

The Schiff base of $pHR_6$ and $pHR_{10}$ is never deprotonated during the photocycle as well as wild-type and T126D *p*HR, which is shown by the lack of formation of the M intermediate (Figure S2 of the Supporting Information). In contrast, the M intermediate appears for all proton-pumping rhodopsins in Figure 5. However, it should be noted that the formation of M is not directly coupled to the proton pumping activity of rhodopsins. Photoexcitation of *Anabaena* sensory rhodopsin (ASR) and *Neurospora* rhodopsin (NR) causes the formation of the M intermediate, but they do not pump protons.[45,46] Therefore, the property to form the M intermediate is not sufficient for rhodopsins to pump protons. Figure 5 clearly shows that neither ASR nor NR possesses a strongly hydrogen bonded water molecule, as we reported previously.[34,47,48] It is thus likely that a strongly hydrogen bonded water molecule is more directly coupled to the proton pumping function.

One question is why such correlation exists, though a water molecule is much smaller in size than the whole protein. In this regard, we note that light energy is first stored in an isomerized form of the retinal chromophore in rhodopsins. A chromophore distorted by photoisomerization has been regarded as the main component of light energy storage for rhodopsins.[49,50] In addition, the observed correlation strongly suggests the importance of the hydrogen bonding network for light energy storage, where the weakened hydrogen bonding network acts as the energy storage component. In fact, the previous QM/MM


dx.doi.org/10.1021/bi300485r | *Biochemistry* 2012, 51, 4677−4684

calculation showed that the amount of light energy stored in a weakened hydrogen bond is larger than that of chromophore distortion in the case of BR.[42] Thus, asymmetric functional conversion between BR and HR can be explained in terms of hydrogen bonds of internal water molecules, the determinant of proton pumps.

## CONCLUSION

A proton pump can be converted into a chloride pump by a single amino acid replacement. In contrast, this study shows that a chloride pump cannot be converted into a proton pump even via the replacement of 6 and 10 amino acids. Light-induced difference FTIR spectroscopy revealed that strongly hydrogen bonded water molecules are not gained for the multiple mutants of pHR, and we concluded that it is the main cause of the lack of functional conversion, because such water molecules are the functional determinants of proton pumps. It has been suggested that the proton pump is the origin of various microbial rhodopsins.[51] If this is true, proton-pumping rhodopsins must have evolved via conservation of the water-containing hydrogen bonding network, whereas other functions may be gained by modifying the hydrogen bonding structures of the active center. These results will be also used for the protein engineering of light-driven pumps for the application of optogenetics in the future.

## ASSOCIATED CONTENT

### Supporting Information

Characteristic amino acid residues of proton and chloride pumps (Figure S1), light-minus-dark difference UV−visible spectra of wild-type and mutant HRs (Figure S2), light-minus-dark difference FTIR spectra of wild-type and mutant HRs (Figure S3), and the isotope effect of the [$\zeta$-$^{15}$N]Lys-labeled sample on the FTIR signal at 2300−2000 cm$^{-1}$ (Figure S4). This material is available free of charge via the Internet at http://pubs.acs.org.

## AUTHOR INFORMATION

### Corresponding Author

*Department of Frontier Materials, Nagoya Institute of Technology, Showa-ku, Nagoya 466-8555, Japan. Phone and fax: 81-52-735-5207. E-mail: kandori@nitech.ac.jp.

### Funding

This work was supported by grants from the Japanese Ministry of Education, Culture, Sports, Science and Technology to H.K. (20108014 and 22247024).

### Notes

The authors declare no competing financial interest.

## REFERENCES

(1) Deisseroth, K. (2011) Optogenetics. *Nat. Methods 8*, 26−29.
(2) Hegemann, P., and Möglich, A. (2011) Channelrhodopsin engineering and expolation of new optogenetic tools. *Nat. Methods 8*, 39−42.
(3) Kato, H. E., Zhang, F., Yizhar, O., Ramakrishnan, C., Nishizawa, T., Hirata, K., Ito, J., Aita, Y., Tsukazaki, T., Hayashi, S., Hegemann, P., Maturana, A. D., Ishitani, R., Deisseroth, K., and Nureki, O. (2012) Crystal structure of the channelrhodopsin light-gated cation channel. *Nature 482*, 369−374.
(4) Zhang, F., Wang, L. P., Brauner, M., Liewald, J. F., Kay, K., Watzke, N., Wood, P. G., Bamberg, E., Nagel, G., Gottschalk, A., and Deisseroth, K. (2007) Multimodal fast optical interrogation of neural circuitry. *Nature 446*, 633−639.
(5) Chow, B. Y., Han, X., Dobry, A. S., Qian, X., Chuong, A. S., Li, M., Henninger, M. A., Belfort, G. M., Lin, Y., Monahan, P. E., and Boyden, E. S. (2010) High-performance genetically targetable optical neural silencing by light-driven proton pumps. *Nature 463*, 98−102.
(6) Haupts, U., Tittor, J., and Oesterhelt, D. (1999) Closing in on bacteriorhodopsin: Progress in understanding the molecules. *Annu. Rev. Biophys. Biomol. Struct. 28*, 367−399.
(7) Lanyi, J. K. (2004) Bacteriorhodopsin. *Annu. Rev. Physiol. 66*, 665−688.
(8) Váró, G. (2000) Analogies between halorhodopsin and bacteriorhodopsin. *Biochim. Biophys. Acta 1460*, 220−229.
(9) Essen, L.-O. (2002) Halorhodopsin: Light-driven ion pumping made simple? *Curr. Opin. Struct. Biol. 12*, 516−522.
(10) Kandori, H. (2011) Protein-Controlled Ultrafast Photoisomerization in Rhodopsin and Bacteriorhodopsin. In *Supramolecular Photochemistry: Controlling Photochemical Processes* (Ramamurthy, V., and Inoue, Y., Eds.) pp 571−596, John Wiley & Sons, Inc., Hoboken, NJ.
(11) Luecke, H., Schobert, B., Richter, H.-T., Cartailler, J. P., and Lanyi, J. K. (1999) Structure of bacteriorhodopsin at 1.55 Å resolution. *J. Mol. Biol. 291*, 899−911.
(12) Kolbe, M., Besir, H., Essen, L.-O., and Oesterhelt, D. (2000) Structure of the light-driven chloride pump halorhodopsin at 1.8 Å resolution. *Science 288*, 1390−1396.
(13) Kouyama, T., Kanada, S., Takeguchi, Y., Narusawa, A., Murakami, M., and Ihara, K. (2010) Crystal structure of the light-driven chloride pump halorhodopsin from *Natronomonas pharaonis*. *J. Mol. Biol. 396*, 564−579.
(14) Sasaki, J., Brown, L. S., Chon, Y.-S., Kandori, H., Maeda, A., Needleman, R., and Lanyi, J. K. (1995) Conversion of bacteriorhodopsin into a chloride ion pump. *Science 269*, 73−75.
(15) Facciotti, M. T., Cheung, V. S., Nguyen, D., Rouhani, S., and Glaeser, R. M. (2003) Crystal structure of the bromide-bound D85S mutant of bacteriorhodopsin: Principles of ion pumping. *Biophys. J. 85*, 451−458.
(16) Shibata, M., Ihara, K., and Kandori, H. (2006) Hydrogen-bonding interaction of the protonated Schiff base with halides in a chloride-pumping bacteriorhodopsin mutant. *Biochemistry 45*, 10633−10640.
(17) Havelka, W. A., Henderson, R., and Oesterhelt, D. (1995) Three-dimensional structure of halorhodopsin at 7 Å resolution. *J. Mol. Biol. 247*, 726−738.
(18) Váró, G., Brown, L. S., Needleman, R., and Lanyi, J. K. (1996) Proton transport by halorhodopsin. *Biochemistry 35*, 6604−6611.
(19) Bamberg, E., Tittor, J., and Oesterhelt, D. (1993) Light-driven proton or chloride pumping by halorhodopsin. *Proc. Natl. Acad. Sci. U.S.A. 90*, 639−643.
(20) Haupts, U., Tittor, J., Bamberg, E., and Oesterhelt, D. (1997) General concept for ion translocation by halobacterial retinal proteins: The isomerization/switch/transfer (IST) model. *Biochemistry 36*, 2−7.
(21) Sato, M., Kanamori, T., Kamo, N., Demura, M., and Nitta, K. (2002) Stopped-flow analysis on anion binding to blue-form halorhodopsin from *Natronomonas pharaonis*: Comparison with the anion-uptake process during the photocycle. *Biochemistry 41*, 2452−2458.
(22) Sato, M., Kubo, M., Aizawa, T., Kamo, N., Kikukawa, T., Nitta, K., and Demura, M. (2005) Role of putative anion-binding sites in cytoplasmic and extracellular channels of *Natronomonas pharaonis* halorhodopsin. *Biochemistry 44*, 4775−4784.
(23) Shibata, M., Muneda, M., Sasaki, T., Shimono, K., Kamo, N., Demura, M., and Kandori, H. (2005) Hydrogen-bonding alterations of the protonated Schiff base and water molecule in the chloride pump of *Natronobacterium pharaonis*. *Biochemistry 44*, 12279−12286.
(24) Shimono, K., Furutani, Y., Kamo, N., and Kandori, H. (2003) Vibrational models of the protonated Schiff base in *pharaonis* phoborhodopsin. *Biochemistry 42*, 7801−7806.
(25) Shibata, M., Yoshitsugu, M., Mizuide, N., Ihara, K., and Kandori, H. (2007) Halide binding by the D212N mutant of bacteriorhodopsin

affects hydrogen bonding of water in the active site. *Biochemistry 46*, 7525−7535.
(26) Yoshitsugu, M., Yamada, J., and Kandori, H. (2009) Color-changing mutation in the E-F loop of propeorhodopsin. *Biochemistry 48*, 4324−4330.
(27) Yamada, K., Kawanabe, A., and Kandori, H. (2010) Importance of alanine at position 178 in proteorhodopsin for absorption of prevalent ambient light in the marine environment. *Biochemistry 49*, 2416−2423.
(28) Muneda, N., Shibata, M., Demura, M., and Kandori, H. (2006) Internal water molecules of the proton-pumping halorhodopsin in the presence of azide. *J. Am. Chem. Soc. 128*, 6294−6295.
(29) Rothschild, K. J., Bousché, O., Braiman, M. S., Hasselbacher, C. A., and Spudich, J. L. (1988) Fourier transform infrared study of the halorhodopsin chloride pump. *Biochemistry 27*, 2420−2424.
(30) Hackmann, C., Guijarro, J., Chizhov, I., Engelhard, M., Rödig, C., and Siebert, F. (2001) Static and time-resolved step-scan Fourier transform infrared investigations of the photoreaction of halorhodopsin from *Natronobacterium pharaonis*: Consequences for models of the anion translocation mechanism. *Biophys. J. 81*, 394−406.
(31) Kandori, H., Belenky, M., and Herzfeld, J. (2002) Vibrational frequency and dipolar orientation of the protonated Schiff base in bacteriorhodopsin before and after photoisomerization. *Biochemistry 41*, 6026−6031.
(32) Shimono, K., Furutani, Y., Kamo, N., and Kandori, H. (2003) Vibrational models of the protonated Schiff base in *pharaonis* phoborhodopsin. *Biochemistry 42*, 7801−7806.
(33) Ikeda, D., Furutani, Y., and Kandori, H. (2007) FTIR study of the retinal Schiff base and internal water molecules of proteorhodopsin. *Biochemistry 46*, 5365−5373.
(34) Kawanabe, A., Furutani, Y., Jung, K.-H., and Kandori, H. (2006) FTIR study of the photoisomerization processes in the 13-cis and all-trans forms of *Anabaena* sensory rhodopsin at 77 K. *Biochemistry 45*, 4362−4370.
(35) Hashimoto, K., Choi, A. R., Furutani, F., Jung, K.-H., and Kandori, H. (2010) Low-temperature FTIR study of *Gloeobacter* rhodopsin: Presence of strongly hydrogen-bonded water and long-range structural protein perturbation upon retinal photoisomerization. *Biochemistry 49*, 3343−3350.
(36) Shibata, M., and Kandori, H. (2005) FTIR studies of internal water molecules in the Schiff base region of bacteriorhodopsin. *Biochemistry 44*, 7406−7413.
(37) Garczarek, F., and Gerwert, K. (2006) Functional waters in intraprotein proton transfer monitored by FTIR difference spectroscopy. *Nature 439*, 109−112.
(38) Wolf, S., Freier, E., Potschies, M., Hofmann, E., and Gerwert, K. (2010) Directional proton transfer in membrane proteins achieved through protonated protein-bound water molecules: A proton diode. *Angew. Chem., Int. Ed. 49*, 6889−6893.
(39) Freier, E., Wolf, S., and Gerwert, K. (2011) Proton transfer via a transient linear water-molecule chain in a membrane protein. *Proc. Natl. Acad. Sci. U.S.A. 108*, 11435−11439.
(40) Kandori, H. (2000) Role of internal water molecules in bacteriorhodopsin. *Biochim. Biophys. Acta 1460*, 177−191.
(41) Kandori, H. (2004) Hydration switch model for the proton transfer in the Schiff base region of bacteriorhodopsin. *Biochim. Biophys. Acta 1658*, 72−79.
(42) Hayashi, S., Tajkhorshid, E., Kandori, H., and Schulten, K. (2004) Role of hydrogen-bond network in energy storage of bacteriorhodopsin's light-driven proton pump revealed by ab initio normal-mode analysis. *J. Am. Chem. Soc. 126*, 10516−10517.
(43) Bogomolni, R. A., Stoeckenius, W., Szundi, I., Perozo, E., Olson, K. D., and Spudich, J. L. (1994) Removal of transducer HtrI allows electrogenic proton translocation by sensory rhodopsin I. *Proc. Natl. Acad. Sci. U.S.A. 91*, 10188−10192.
(44) Sudo, Y., Iwamoto, M., Shimono, K., Sumi, M., and Kamo, N. (2001) Photo-induced proton transport of *pharaonis* phoborhodopsin (sensory rhodopsin II) is ceased by association with the transducer. *Biophys. J. 80*, 916−922.
(45) Sineshchekov, O. A., Spudich, E. N., Trivedi, V. D., and Spudich, J. L. (2006) Role of the cytoplasmic domain in *Anabaena* sensory rhodopsin photocycling: Vectoriality of Schiff base deprotonation. *Biophys. J. 91*, 4519−4527.
(46) Brown, L. S., Dioumaev, A. K., Lanyi, J. K., Spudich, E. N., and Spudich, J. L. (2001) Photochemical reaction cycle and proton transfers in *Neurospora* rhodopsin. *J. Biol. Chem. 276*, 32495−32505.
(47) Furutani, Y., Kawanabe, A., Jung, K.-H., and Kandori, H. (2005) FTIR spectroscopy of the all-trans form of *Anabaena* sensory rhodopsin at 77 K: Hydrogen bond of a water between the Schiff base and Asp75. *Biochemistry 44*, 12287−12296.
(48) Furutani, Y., Bezerra, A. G., Jr., Waschuk, S., Sumii, M., Brown, L. S., and Kandori, H. (2004) FTIR spectroscopy of the K photointermediate of *Neurospora* rhodopsin: Structural changes of the retinal, protein, and water molecules after photoisomerization. *Biochemistry 43*, 9636−9646.
(49) Birge, R. R. (1990) Nature of the primary photochemical events in rhodopsin and bacteriorhodopsin. *Biochim. Biophys. Acta 1016*, 293−327.
(50) Kukura, P., McCamant, D. W., Yoon, S., Wandschneider, D. B., and Mathies, R. A. (2005) Structural observation of the primary isomerization in vision with femtosecond-stimulated Raman. *Science 310*, 1006−1009.
(51) Sharma, A. K., Spudich, J. L., and Doolittle, W. F. (2006) Microbial rhodopsins: Functional versatility and genetic mobility. *Trends Microbiol. 14*, 463−469.
(52) Mizuide, N., Shibata, M., Friedman, N., Sheves, M., Belenky, M., Herzfeld, J., and Kandori, H. (2006) Structural changes in bacteriorhodopsin following retinal photoisomerization from the 13-*cis* form. *Biochemistry 45*, 10674−10681.
(53) Shibata, M., Yoshitsugu, M., Mizuide, N., Ihara, K., and Kandori, H. (2007) Halide binding by the D212N mutant of bacteriorhodopsin affects hydrogen bonding of water in the active site. *Biochemistry 46*, 7525−7535.
(54) Suzuki, D., Sudo, Y., Furutani, Y., Takahashi, H., Homma, M., and Kandori, H. (2008) Structural changes of *Salinibacter* sensory rhodopsin I upon formation of the K and M photointermediates. *Biochemistry 47*, 12750−12759.
(55) Kandori, H., Furutani, Y., Shimono, K., Shichida, Y., and Kamo, N. (2001) Internal water molecules of *pharaonis* phoborhodopsin studied by low-temperature infrared spectroscopy. *Biochemistry 40*, 15693−15698.
(56) Sumii, M., Furutani, Y., Waschuk, S. A., Brown, L. S., and Kandori, H. (2005) Strongly hydrogen-bonded water molecule present near the retinal chromophore of *Leptosphaeria* rhodopsin, bacteriorhodopsin-like proton pump from a eukaryote. *Biochemistry 44*, 15159−15166.
(57) Furutani, Y., Shichida, Y., and Kandori, H. (2003) Structural changes of water molecules during the photoactivation processes in bovine rhodopsin. *Biochemistry 42*, 9619−9625.
(58) Ota, T., Furutani, Y., Terakita, A., Shichida, Y., and Kandori, H. (2006) Structural changes in the Schiff base region of squid rhodopsin upon photoisomerization studied by low-temperature FTIR spectroscopy. *Biochemistry 45*, 2845−2851.
(59) Katayama, K., Furutani, Y., Imai, H., and Kandori, H. (2012) Protein-bound water molecules in primate red- and green-sensitive visual pigments. *Biochemistry 51*, 1126−1133.
(60) Shibata, M., Muneda, N., Ihara, K., Sasaki, T., Demura, M., and Kandori, H. (2004) Internal water molecules of light-driven chloride pump proteins. *Chem. Phys. Lett. 392*, 330−333.